5. Garner, F. H., and A. B. Hale, *ibid.*, **2**, 157 (1953).
6. Garner, F. H., and T. T. Lane, *Trans. Inst. Chem. Eng. (London)*, **37**, 162 (1959).
7. Davies, J. T., "Advances in Chemical Engineering," pp. 1-50, Academic Press, New York (1963).
8. Savic, P., *Natl. Res. Lab. Rept. (Canada) MT-22* (1953).
9. Kinter, R. C., "Advances in Chemical Engineering," pp. 52-92, Academic Press, New York (1963).
10. Davies, J. T., A. A. Kilmer, and G. A. Ratcliff, *Chem. Eng. Sci.*, **19**, 483 (1964).
11. Davies, J. T., and G. R. A. Mayers, *ibid.*, **16**, 55 (1961).
12. Bayens, C., unpublished paper, Chem. Eng. Dept., Johns Hopkins Univ.
13. Gal-Or, Benjamin, D.Sc. thesis, Technion, Israel Inst. Technol. (in Hebrew) (1964).
14. ———, and William Resnick, *Chem. Eng. Sci.*, **19**, 653 (1964).
15. Olney, R. B., *A.I.Ch.E. J.*, **10**, 827 (1964).
16. Hadamard, J., *Compt. Rend. Acad. Sci. Paris*, **152**, 1735 (1911).
17. Rybczynski, W., *Bull. Intern. Acad. Sci. Cracovie* (A), 40 (1911).
18. Gal-Or, Benjamin, and William Resnick, *A.I.Ch.E. J.*, **11**, 740 (1965).
19. Swift, I. L., and S. K. Friedlander, *J. Colloid Sci.*, **19**, 621 (1964).
20. Hanratty, T. J., *A.I.Ch.E. J.*, **2**, 359 (1956).
21. Deindoerfer, F. H., and A. Humphrey, *Ind. Eng. Chem.*, **53**, 755 (1961).
22. Calderbank, P. H., *Trans. Inst. Chem. Engrs.*, **37**, 173 (1959).
23. Gal-Or, Benjamin, and William Resnick, *Ind. Eng. Chem. Process Design Development*, **5**, 15 (1966); *ibid.*, to be published.
24. Toor, H. L., and T. M. Marchello, *A.I.Ch.E. J.*, **4**, 97 (1958).
25. Gal-Or, Benjamin, *A.I.Ch.E. J.*, **12**, No. 3 (1966).

APPENDIX

Mean volume radius is defined as

$$a_v = \sqrt[3]{\frac{\sum_{i=1}^{Nv\ Vv} n_i a_i^3}{\sum_{i=1}^{Nv\ Vv} n_i}} \tag{A1}$$

However, in many cases the average particle radius is evaluated experimentally by measuring of dispersed phase holdup and total area of dispersed particles A and by expressing the results as

$$a_{32} = \frac{3[\text{Holdup vol.}]}{A} \tag{A2}$$

It should be noted that Equation (A2) gives the surface mean radius which is defined as

$$a_{32} = \frac{\sum_{i=1}^{Nv\ Vv} n_i a_i^3}{\sum_{i=1}^{Nv\ Vv} n_i a_i^2} = \frac{3\Phi}{A/Vv} = \frac{3[\text{Holdup vol.}]}{A} \tag{A3}$$

By the use of Equation (14) and (32), Equation (A3) gives

$$a_{32} = \frac{\int_0^\infty a^3 f^\circ(a, \bar{a}_v)\, da}{\int_0^\infty a^2 f^\circ(a, \bar{a}_v)\, da} = \frac{\Gamma(3.0)}{\Gamma(2\frac{1}{2})^{\alpha 1/2}} = 1.148\bar{a}_v \tag{A4}$$

Manuscript received April 30, 1965; revision received October 4, 1965; paper accepted December 3, 1965. Paper presented at A.I.Ch.E. Philadelphia meeting.

Longitudinal Dispersion in Rotating Impeller Types of Contactors

TERUKATSU MIYAUCHI, HIROMI MITSUTAKE, and ICHIRO HARASE

University of Tokyo, Tokyo, Japan

On the basis of a back-flow model, the rates of interstage mixing of continuous phase for RDC and Mixco columns are measured experimentally under flow and nonflow conditions. These rates are correlated into dimensionless formulas for wide combinations of operational condition, column geometry, and dimensions, and are put into a single formula by introducing the power number as an additional parameter. The final correlation covers the impeller Reynolds number from 3.5×10^3 to 1.0×10^6 and the diameter of columns from 4.1 to 218 cm.

Longitudinal dispersion coefficients for continuous phase in the rotating shaft types of columns have been investigated here experimentally to interpret the extraction behavior of the contactors along the concept presented for two-phase counterflow operations with longitudinal dispersion (*1, 5, 7, 8, 16, 19, 20, 23, 28*). Two types of contactors are investigated: the rotating disk contactor (RDC) introduced by Reman and Olney (*14*), and the Mixco column of Oldshue and Rushton (*13*).

Hiromi Mitsutake, and Ichiro Harase are with Chiyoda Chemical Engineering and Construction Co., Ltd., Tokyo, Japan.

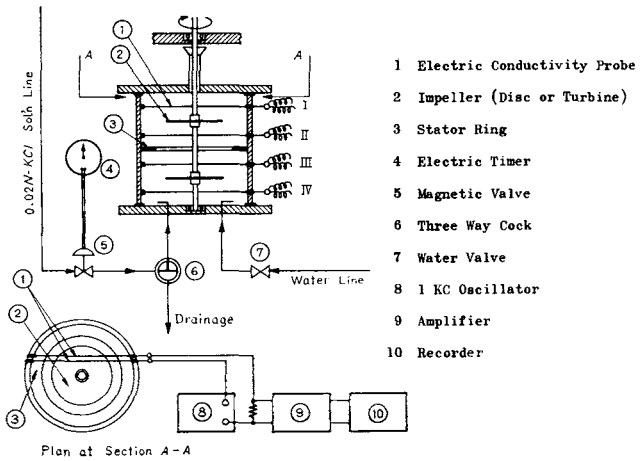

Fig. 1. Schematic diagram of nonflow, two-stage column.

These contactors utilize considerably different mixing devices for droplets dispersion, that is, rotating disks under unbaffled condition for the former, and turbine impellers under fully baffled condition for the latter.

Many measurements have been presented for longitudinal dispersion in RDC (*2, 12, 21, 22, 24, 26, 27*). The influence of column geometry on the coefficient, however, is limited in these measurements. The apparent coefficients for continuous phase have also been reported (*9, 29*) for other rotating shaft types of contactors, including the Mixco columns. According to the back-flow model concept (*4, 8, 24*), the longitudinal dispersion coefficient E_c for continuous phase is expressed as follows (*6, 8*):

$$E_c = \epsilon_c E = \frac{\overline{F}_c L_o}{2\beta - 1/n_p} + \frac{F_c L_o}{\beta} \qquad (1)$$

where β is a superficial number of perfectly mixed stages in series in each compartment and E is the coefficient for the mixed phases. Equation (1) simplifies further when $F_c = \epsilon_c F$, where F is the superficial rate of interstage mixing of the mixed phases. The equation, with $\beta = 1$, is then reduced to the relation presented experimentally for RDC (*22*).

To measure E experimentally, continuous multistage columns are operated, with transient injection of electrolyte solution as a tracer. For determining experimental F, simple two-stage columns are utilized under nonflow condition with transient injection of the tracer. This latter experimental method is particularly advantageous in measuring F in geometrically dissimilar columns and utilized extensively in the following steps. F is then reduced to E and vice versa from the use of Equation (1).

EXPERIMENTAL APPARATUS AND PROCEDURES

Nonflow, Two-Stage Experiment for *F*

Experimental Apparatus. The assembly of the entire apparatus is shown in Figure 1. It consists of constant level feed vessels of water, and 0.02N aqueous solution of potassium chloride as tracer electrolytes; and the two-stage main column, stainless steel wire electrodes for detecting concentration change of tracer electrolyte, 1.0 kilocycle a.c. oscillator, a four-channel amplifier for measuring electrode circuit current, and a pen-writing recorder. The range of experimental variables is summarized in Table 1. The column is essentially a two-compartment mixing vessel with a brass stator ring at the midheight of the vessel. Two brass impellers (rotating disks in the case of the figure) with a 10-mm. diameter common brass shaft are located centrally in each compartment. All the surfaces exposed to the vessel liquor are protected with insulating varnish, except the electrodes. Four pairs of electrodes are horizontally inserted in the vessel, each pair consisting of two parallel stainless steel 0.6 mm. diameter wires 5.0 mm. apart, as shown in the plan at the section A-A.

Experimental Procedures. First the vessel is filled with water, and after steady state is reached, a certain amount of potassium chloride solution is fed as a concentration impulse through the bottom plate inlet. The concentration in the lower compartment increases rapidly to a certain point, gradually decreasing thereafter, and that in the upper compartment increases gradually as shown in Figure 4. If the liquid in each compartment is mixed perfectly, the readings of two pairs of conductivity probes located in one compartment should give the same value. Usually they are different slightly, particularly in the range of lower rotation speed of impellers. A mean value is adopted for analyzing the data recorded to get F.

TABLE 1. SUMMARY OF EXPERIMENTAL VARIABLES

1-1 Non-flow two-stage column runs:

Experimental variables	RDC	Mixco columns
Diameter of column; D_T, (cm.)	10 - 30	15 - 30
Area ratio of stator opening: $(D_s/D_T)^2$, (-)	0.19 - 1.0	0.19 - 1.0
Height ratio of compartment : L_o/D_T, (-)	0.2 - 0.93	0.2 - 0.93
Dia. ratio of impeller : d/D_T, (-)	1/3 - 2/3	1/3
Reynolds number studied : nd^2/ν, (-)	$(0.98\text{-}42)\times10^4$	$(0.9\text{-}8.8)\times10^4$

1-2 Continuous-flow multistage column runs:

a. Rotating disc contactors

Investigators	D_T cm	$\frac{D_s}{D_T}$	$\frac{d}{D_T}$	$\frac{L_o}{D_T}$	$\overline{F}_c$ cm/s	$\overline{F}_d$ cm/s	$(\frac{nd^2}{\nu})\times10^{-4}$
Present Investigation	15	0.72	0.50	0.50	0.037-0.050	0	2.63-18.6
					0.009-0.020	0.013-0.057	1.40-9.30
Oshima (12)	9.1	0.72	0.50	0.51	0.026-0.274	0	2.7-10.8
					0.095-0.229	0.059-0.276	0.74-3.38
Kagan et al (2)+	20	0.85	0.80	0.50	0.141-0.462	0	8.6-28.6
Stemerding, Lumb & Lips (24)*+	6.4	0.74	0.66	0.31	0.06 -.0.57	0	0.35-4.98
	30	0.70	0.63	0.33	0.39 - 1.57	0	4.5 - 16.9
	64	0.66	0.50	0.20	0.22 - 0.85	0	8.4-40.8
	218	0.71	0.46	0.12	0.30 - 0.60	0	52.5-102.5
Westerterp & Landsman (26)	4.1	0.73	0.49	0.61	0.018-0.139	0	0.80
	5.0	0.74	0.58	0.42	0.010-0.181	0	0.42-2.52
Stainthorp et al (21)	3.5	0.63	0.50	0.54	-	-	-
Strand, Olney & Ackerman (22)	10.1	0.75	0.50	0.50			
	15.2	0.66	0.50	0.35	-	-	-
	105	0.79	0.51	0.24			

* The data plotted in Figures 5 and 7 are read from the smoothed curves given in the original Figures, so that the points plotted here do not necessarily correspond to the individual original experimental points, but they rather express selected points to give averaged behavior of the columns.

\+ The data of these investigators are read from the original Figures, so that there are some questions on the accuracy of numerical values listed here.

b. Mixco columns

Investigators	D_T (cm)	$\frac{D_s}{D_T}$	$\frac{d}{D_T}$	$\frac{L_o}{D_T}$	$\overline{F}_c$(cm/s)	$\overline{F}_d$(cm/s)	$(\frac{nd^2}{\nu})\times10^{-4}$
Present Investigation	15	0.43	0.33	0.50	0.004-0.074	0	0.35-6.67
	15	0.50	0.33	0.50	0.009-0.036	0 - 0.057	0.77-2.61
Yagi & Miyauchi (29)	15	0.43-1.0	0.34	0.43	0.040-0.087	0	1.04-2.60
	15	0.43	0.34	0.80	0.048	0	1.33-2.58

Continuous Multistage Column Experiment for *E*

Experimental Apparatus. The assembly of the entire apparatus, and the underlying principles and method of measuring the longitudinal dispersion coefficient for continuous phase are essentially the same as those utilized previously for pulsed perforated plate columns (*6*), except for the main column and the location of conductivity probes.

Details of the main column are illustrated in Figure 2 (Mixco type of column in this case). The column is constructed from a 150 mm. I.D. Pyrex trubore glass pipe, 1,210 mm. long. When operated for single-phase flow the column is divided into fifteen compartments by fifteen equally spaced brass stator rings. In the case of two-phase counterflow operation, the bottom compartment is used as the droplets disengaging section as shown in Figure 2. The rotor shaft is a 15-mm. brass rod to which are attached brass disks or four flat bladed brass turbines. When the column is operated as the Mixco column, four vertical brass baffles, 10 mm. wide, are attached to the inner surface of the column. The shape and dimensions of the four flat bladed turbine are the same as those reported by Oldshue and Rushton (*13*).

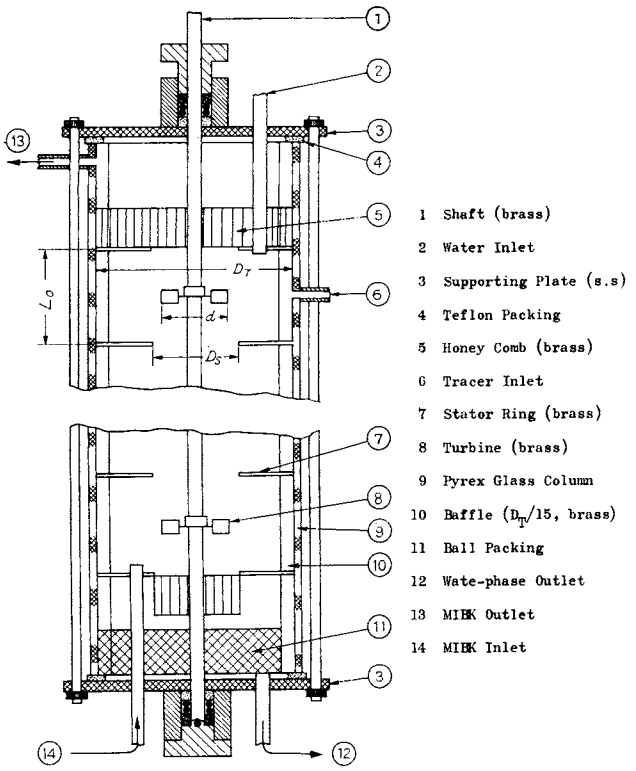

Fig. 2. Detail of continuous multistage column (Mixco).

Experimental Procedures. The procedures are nearly the same as those stated before (6). Aqueous phase is always continuous and MIBK phase is dispersed. The range of the operating variables is shown in Table 1. The tracer solution is introduced into the top compartment as a concentration impulse, and concentration change at the aqueous phase outl is recorded to obtain the response. The response curves are well expressed by the one-dimensional diffusion model.

Analysis of Response Curve

Nonflow Two-Stage Experiment. As shown schematically in Figure 3, the tracer electrolyte of concentration c_t is introduced by v_t cc. into the lower compartment as a concentration impulse at time $\theta = 0$. The concentrations c_1 and c_2 of lower and upper compartments, respectively, start to change with time, and the change is expressed by the following equations, where the content is assumed being mixed perfectly in each compartment:

$$c_1/c_{10} = (1/2)(1 + e^{-2\psi})$$
$$c_1/c_{10} = (1/2)(1 + e^{-2\psi}) \qquad (2)$$

where $\psi = \theta/\theta_m$, $\theta_m = L_o/F$, $c_{10} = (c_t v_t)/(\pi D_T^2 L_o/4)$, and $F = (D_S/D_T)^2 f$. f is the mean rate of interstage mixing of fluid across the stator opening. $(2c_1/c_{10} - 1)$ and $(1 - 2c_2/c_{10})$ are plotted, respectively, against time on a semi-logarithmic scale and the gradients of the lines connecting the data give θ_m immediately.

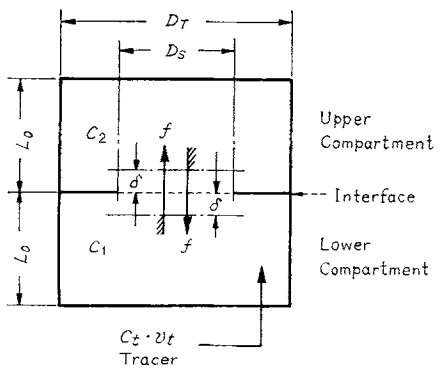

Fig. 3. Nonflow, two-stage operation.

Continuous Multistage Column Experiment. The basic transient equation, appropriate initial and boundary conditions, and the detail of analyzing the experimental delta response curves have all been described previously (6).

RESULTS

An example of nonflow, two-stage transient measurement is shown in Figure 4. The assumption of perfect mixing in each compartment is reasonable. The correspondence of one compartment to one stage means $\beta = 1$ in Equation (1). This is always true in the nonflow runs, but not always true in the continuous column runs. As obvious from Figures 1 and 3, wall resistance to the mean circulating flow in each compartment is not necessarily symmetrical with respect to the impeller sweeping surface for the two-stage columns. The top and bottom plates tend to give higher flow resistance than the stator, with a higher rate of liquid mixing across the sweeping surface. This is not the case for the multistage columns. All the dispersion data are expressed in terms of f. Longitudinal dispersion coefficients obtained from the continuous column runs are also reduced to f by applying Equation (1) with $\beta = 1$. As obvious from Equation (1), the correlation with f is a more severe test of experimental accuracy than that with E. When the column is operated in two-phase counterflow, the kinematic viscosity ν of the mixed phases is taken as (25)

$$\nu = \mu_m/\rho_m$$

with

$$\rho_m = \rho_c \epsilon_c + \rho_d \epsilon_d,$$

and

$$\mu_m = (\mu_c/\epsilon_c)\,[1 + 1.5\,\mu_d \epsilon_d/(\mu_c + \mu_d)].$$

Rotating Disk Contactors

Experimental f is determined, with the nonflow, two-stage columns with wide combinations of column geometry, dimensions, and operational conditions (about one hundred twenty runs). Also, single-phase flow (about fifteen runs) as well as two-phase counterflow experiments (twenty-four runs) are performed for the continuous multistage column, with MIBK as dispersed phase in the latter runs. The hold-up of MIBK in the column ranges from 0 to 18% (mostly several percent or less). The rate of interstage mixing F_c measured experimentally for two-phase runs is converted to f by the following relation:

$$F = F_c/\epsilon_c \quad \text{or} \quad f = f_c/\epsilon_c \qquad (3)$$

All the data for both the flow and nonflow runs agree fairly well when expressed by the following dimensionless equation. The correlations for various geometrically dissimilar columns are within the accuracy of data for each particular column, as shown in Figure 5.*

$nd^2/\nu > 1.2 \cdot 10^5$:

$$f/nd = 4.3 \cdot 10^{-3}\,(D_T/L_o)^{1/2}\,(D_T/D_s)^{1/4} \qquad (4a)$$

$nd^2/\nu < 1.2 \cdot 10^5$:

$$f/nd = 4.5 \cdot 10^{-2}\,(D_T/L_o)^{1/2}\,(D_T/D_s)^{1/4}\,(nd^2/\nu)^{-1/5} \qquad (4b)$$

Mixco Columns

Experimental f is determined with the nonflow, two-stage columns (about seventy runs). The data are well correlated by the following equation as shown in Figure 6.*

* Figures 5 through 8 have been deposited as document 8765 with the American Documentation Institute, Photoduplication Service, Library of Congress, Washington 25, D. C., and may be obtained for $2.50 for photoprints or $1.75 for 35-mm. microfilm.

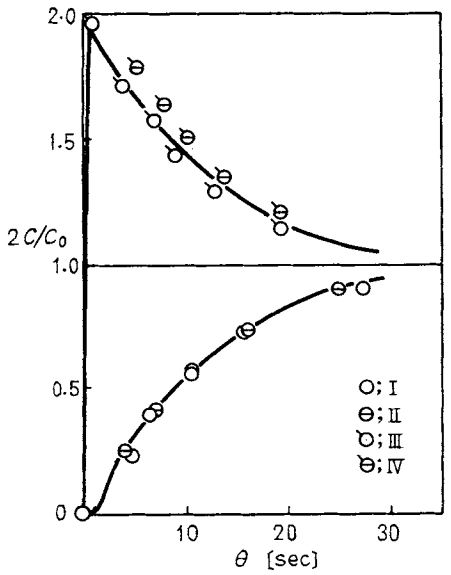

Fig. 4. Transient change of concentration in two-stage column. (The numbering of the data points corresponds to that given to the four conductivity probes shown in Figure 1.) Two-stage Mixco column with four vertical baffles 1.0 cm. wide. D_T = 15 cm., D_s = 6.5 cm., d = 5.0 cm., L_o = 7.5 cm., and 685 rev./min.

$$f/nd = 2.7 \cdot 10^{-2} \, (D_T/L_o)^{1/2} \qquad (5a)$$

Also the continuous multistage column is operated under single-phase flow (about seventy runs) as well as two-phase counterflow (twenty-four runs). Hold-up of dispersed phase ranges from 0 to 60%. To calculate f_c from the experimental E_c, β included in Equation (1) is always assumed equal to 1.0. The plotting of data in Figure 6 shows that f for the continuous column deviates from the upper branch, Equation (5*a*), at $nd^2/\nu \approx 2 \cdot 10^4$, and gradually approaches the lower branch, Equation (5*b*), with decreasing nd^2/ν. The lower branch ($nd^2/\nu \lesssim 1.0 \cdot 10^4$) is expressed by

$$f/nd = 1.0 \cdot 10^{-2} \, (D_T/L_o)^{1/2} \qquad (5b)$$

This branch suggests that each compartment behaves more likely as nearly two-stages in series ($\beta \approx 2$) for $nd^2/\nu \leq 10^4$.

DISCUSSION OF RESULTS

The above correlations show that f/nd is proportional to $(D_T/L_o)^{1/2}$ for both the RDC and the Mixco columns, with small corrections of (D_T/D_s) and (nd^2/ν) for the former. The correlations reported previously are easily modified to equations similar to (4) and (5). Thus the correlation by Strand et al. (22), Stemerding et al. (24), and Westerterp and Landsman (26) simplify to

$$f/nd \doteq 0.012 \qquad (6)$$

The data by Westerterp and Landsman, and Stemerding et al, are recalculated to give f from the use of Equation (1) with $\beta = 1$ and $\epsilon_c = 1$, and are plotted in Figure 7.* Their fd/ν obviously depends on nd^2/ν in essentially the same way as ours. The measurements by Oshima (12) for a 9.1-cm. diameter column are about 30% lower than ours, perhaps due to end effect. The data available from Kagan et al. (2) for a 20-cm. diameter column fairly scatter and no further comparison is made. The correlation by the present authors cover all the data reasonably well for the entire range of variables.

For the Mixco column fairly limited data are available (29). These are recalculated to get f and plotted in Figure 8.* The column with a higher compartment (L_o/D_T = 1.0) behaves as $\beta \approx 2$, and those with lower compartments (L_o/D_T = ½) give about 40% higher coefficients than ours, possibly due to slight mallocation of turbines.

EXTENSION OF RESULTS

The column structure and mixing devices for RDC are considerably different from those of Mixco columns. The correlation already obtained are extended here to put them into a single correlation, with the dual purpose of first making clear the underlying mechanisms of interstage mixing, and second of giving a reasonable basis for predicting the rate of interstage mixing in a column with various combinations of column geometry and the type of impeller.

Interstage Mixing and Turbulent Diffusion

Under a steady state operation of a column, the net rate N of interstage mixing between two adjacent compartments across the opening of the stator ring is given by

$$N = (\pi D_s^2/4) \, f \, (c_1 - c_2) \qquad (7)$$

where c_1 and c_2 are shown in Figure 3. f is seen to be equivalent to the overall coefficient of mass transfer for the two turbulent films formed on both sides of the interstage interface. Flow pattern in the adjacent compartments is symmetrical with respect to the interface, so that the thickness δ of the films is the same. Let $\overline{E}_\lambda$ be the mean turbulent diffusion coefficient effective to the interstage mixing. f is combined with E_λ and δ as follows:

$$1/f = \delta/\overline{E}_\lambda + \delta/\overline{E}_\lambda \quad \text{or} \quad f = E_\lambda/2\delta \qquad (8)$$

Turbulent Diffusion Coefficient

When the flow condition of fluid in each compartment is under a developed turbulence, turbulent diffusion in the fluid is considered to be governed by ϵ_o, the mean rate of energy dissipation per unit mass of the fluid.

Under the premise that the concept of Kolmogoroff's local isotropy is applicable to the steady turbulent field in the compartment, the turbulent diffusion in it is the integral effect of the contribution from the all eddies whose wavelengths are smaller† than λ. The eddies greater than λ contribute to the mean circulating flow, and therefore the compartment is rapidly mixed perfectly. With this premise the turbulent diffusion coefficient $\overline{E}_\lambda$ is given (3, 11) by

$$\overline{E}_\lambda = a \, \epsilon_o^{1/3} \, \lambda^{4/3} \qquad (9)$$

where a is a constant and ϵ_o is calculated from the knowledge on the power consumption in mixing vessels (17):

$$\epsilon_o = (N_p \rho n^3 d^5) \Big/ \left(\frac{\pi}{4} D_T^2 L_o \rho\right) \qquad (10)$$

From Equations (8) through (10) the following relation is obtained:

$$f/nd = b \, N_p^{1/3} \, (D_T/L_o)^{1/2} \qquad (11)$$

where

* See footnote on page 510.

* See footnote on page 510.

† The wavelength λ thus defined is considered to be located somewhere in the transition region from the lowest frequency range to the medium frequency range (inertial subrange) in the turbulent eddy spectrum (11).

$$b = \frac{a}{(2\pi)^{1/3}} \cdot \left(\frac{L_o}{D_T}\right)^{1/6} \cdot \left(\frac{d^{2/3}\,\lambda^{4/3}}{D_T\,\delta}\right) \qquad (12)$$

The coefficient b includes two unknown quantities of λ and δ; thus it is a function of Reynolds number and the dimensions of the column. The geometrical factor included in b, $(L_o/D_T)^{1/6}\ (d^{2/3}/D_T)$, changes in its magnitude more than five times, depending upon the column utilized. On the other hand, when Equation (11) is compared with Equations (4) and (5), b seems nearly constant in spite of considerable difference in column design for the RDC and the Mixco columns. If so, the plot of $(fd/\nu)/N_p^{1/3}\ (D_T/L_o)^{1/2}$ against nd^2/ν should give, as obvious from Equation (11), a single straight line on a logarithmic scale for both types of contactors. These parameters are preferred to avoid crowded plotting.

The plot for the most data available is shown in Figure 9. The correlation seems good, with b constant at an average of 0.017. The diameter of the columns correlated here ranges from 4.1 to 218 cm. for the RDC and from 15 to 30 cm. for the Mixco columns. The final correlation thus obtained is

$$f/nd = 0.017\,N_p^{1/3}\,(D_T/L_o)^{1/2} \qquad (13)$$

where N_p for the rotating disks is taken from the work by Nece and Daily (*10*), and is shown in Figure 10, with L_o/d as a parameter. N_p, the turbine impeller, is estimated as 3.8 from the work by Rushton et al. (*17*).

More works are needed to know why b remains nearly unchanged, and the mechanisms of turbulent diffusion in the transition region from the lowest frequency range to the inertial subrange. The constancy of b has been ob-

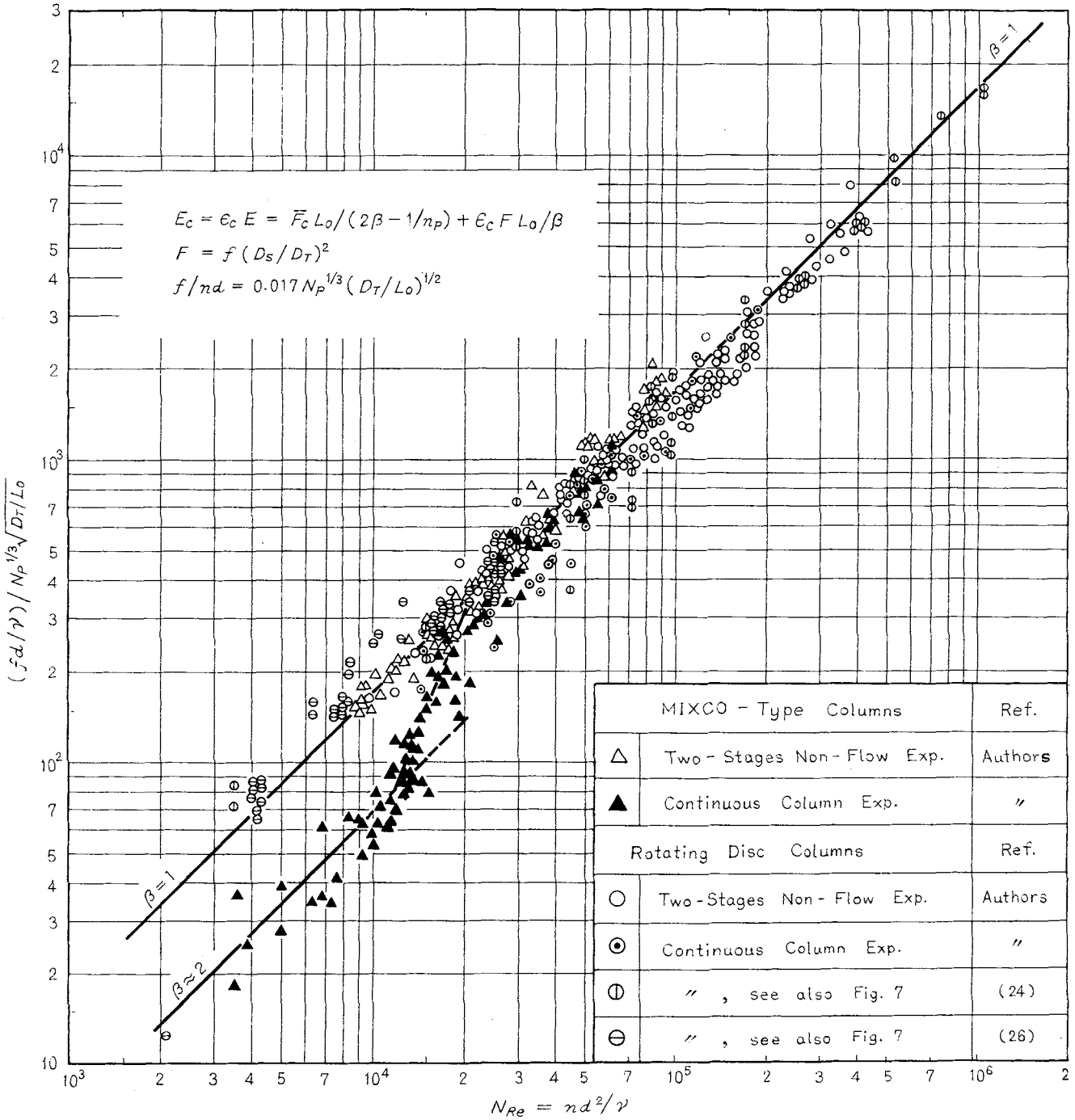

Fig. 9. Unified correlation for both of RDC and Mixco columns.

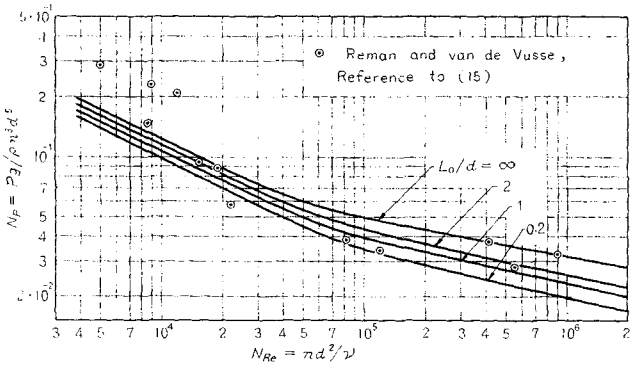

Fig. 10. Power number for rotating disk taken from Nece and Daily (10) [for the applicability of the curves, see also Schlichting (18)].

tained for the columns in which mixing devices as well as power numbers are different. Accordingly, Equation (13) is considered to give a reasonable basis for predicting the rate of interstage mixing for various combinations of column geometry and mixer design.

CONCLUSIONS

1. The rate of interstage mixing between two adjacent compartments in the RDC and the Mixco columns have been measured experimentally by varying the operational conditions, geometry, and dimensions of the columns. Equations (4) and (5) are the dimensionless correlations obtained and are compared with the published data and give a reasonable average for them.

2. On the basis of the physical factors which govern the turbulent diffusion in a mixing vessel, the correlations developed as above semiempirically are put into a single correlation, Equation (13). This correlation is considered reasonable to predict the rate of interstage mixing for a given centrally agitated column.

NOTATION

a = constant, dimensionless
b = constant, dimensionless
c_i = concentration of i^{th} compartment, mole/cc.
c_t = concentration of tracer liquor, mole/cc.
c_{10} = initial concentration [Equation (2)], mole/cc.
D_T = I.D. of column, cm.
D_s = opening diameter of stator ring, cm.
d = diameter of disk or turbine impeller, cm.
E = superficial longitudinal dispersion coefficient, sq. cm./sec.
$\overline{E}_\lambda$ = mean turbulent diffusion coefficient, sq. cm./sec.
F = superficial rate of interstage mixing, cc./(sq. cm.) (sec.)
$\overline{F}$ = superficial flow rate of main stream, cc./(sq. cm.) (sec.)
f = mean actual rate of interstage mixing, cc./(sq. cm.) (sec.)
g = gravitational acceleration, cm./sec.^{2}
L = column height, cm.
L_o = height of one compartment, cm.
N_p = power number, dimensionless
n = rotation speed of disk or impeller, rotation/sec.
n_p = number of stages in series, dimensionless
v_t = volume of trace liquor introduced as a pulse, cc.

Greek Letters

β = factor included in Equation (2), dimensionless
δ = thickness of turbulent film, cm.
ϵ_i = volume fraction of phase i, dimensionless ($i = c$ and d)
ϵ_o = rate of energy dissipation per unit mass of fluid, erg/(g.)(sec.)
θ = time, sec.
θ_m = L_o/F, sec.
λ = maximum wavelength of eddy responsible to eddy diffusion, cm.
μ_i = viscosity of phase i, poise ($i = c$ and d)
μ_m = mean viscosity of mixed phases, poise
ν = kinematic viscosity, stokes
ρ = density of fluid, g./cc.
ρ_i = density of phase i, g./cc. ($i = c$ and d)
ρ_m = mean density of mixed phases, g./cc.
ψ = θ/θ_m, dimensionless

Subscripts

c = continuous phase
d = dispersed phase
i = phase i
m = usually for mixed phases

LITERATURE CITED

1. Hennico, A., G. Jacques, and Theodore Vermeulen, *U. S. Atomic Energy Comm. Rept. UCRL-10696* (1963).
2. Kagan, S. Z., T. B. Bolkoba, and M. E. Aerob, *Chem. Ind. USSR*, No. 12, 39 (1961).
3. Levich, V. G., "Physicochemical Hydrodynamics," 2 ed., Chap. 1 and 3, translated by Scripta Technica, Prentice-Hall, Englewood Cliffs, N. J. (1962).
4. Latinen, G. A., and F. D. Stockton, paper presented at A.I.Ch.E. St. Paul, Minnesota, meeting (September, 1959).
5. Miyauchi, Terukatsu, *U. S. Atomic Energy Comm. Rept. UCRL-3911* (1957).
6. ———, and Haruhiko Oya, *A.I.Ch.E. J.*, **11**, 395 (1965).
7. Miyauchi, Terukatsu, and Theodore Vermeulen, *Ind. Eng. Chem. Fundamentals*, **2**, 113 (1963).
8. *Ibid.*, 304.
9. Nagata, S., W. Eguchi, H. Kasai, and J. Morino, *Chem. Eng. Japan*, **21**, 784 (1957).
10. Nece, R. E., and J. W. Daily, *Trans. Am. Soc. Mech. Engrs., J. Basic Sci.*, **D82**, 562 (1960).
11. Ogura, Yoshimitsu, "Atmospheric Turbulence," 1 ed., Chijin Book Co., Tokyo (1955).
12. Oshima, Tasuku, B.S. thesis, Univ. Tokyo (April, 1960).
13. Oldshue, J. Y., and J. H. Rushton, *Chem. Eng. Progr.*, **48**, 297 (1952).
14. Reman, G. H., and R. B. Olney, *ibid.*, **51**, 141 (1955).
15. Reman, G. H., and J. G. van de Vusse, in "Liquid Extraction," 2 ed., p. 512, McGraw-Hill, New York (1963).
16. Rod, Vladimir, *Brit. Chem. Eng.*, **9**, 300 (1964).
17. Rushton, J. H., E. W. Costich, and H. J. Everett, *Chem. Eng. Progr.*, **46**, 467 (1950).
18. Schlichting, Hermann, "Boundary Layer Theory," translated by J. Kestin, 4 ed., p. 547, McGraw-Hill, New York (1960).
19. Sleicher, C. A., Jr., *A.I.Ch.E. J.*, **5**, 149 (1959).
20. *Ibid.*, **6**, 529 (1960).
21. Stainthorp, E. P., and N. Sudall, *Trans. Inst. Chem. Engrs. London*, **42**, T 198 (1964).
22. Strand, C. P., R. B. Olney, and G. H. Ackerman, *A.I.Ch.E. J.*, **8**, 252 (1962).
23. Stemerding, S., and F. J. Zwiderweg, *Chem. Engs.*, **168**, CE 156 (1963).
24. Stemerding, S., E. C. Lumb, and J. Lips, *Chem.-Ing.-Tech.*, **35**, 844 (1963).
25. Treybal, R. E., "Liquid Extraction," 2 ed., p. 415, McGraw-Hill, New York (1963).
26. Westerterp, K. R., and P. Landsman, *Chem. Eng. Sci.*, **17**, 363 (1962).
27. Westerterp, K. R., and W. H. Meyberg, *ibid.*, 373.
28. Wilburn, N. P., *Ind. Eng. Chem. Fundamentals*, **3**, 189 (1964).
29. Yagi, Sakae, and Terukatsu Miyauchi, *Chem. Eng. Japan*, 507 (1955).

Manuscript received October 4, 1965; revision received December 21, 1965; paper accepted December 23, 1965.